PROCEEDINGS OF SCIENCE

Seasonal variation of atmospheric muons

Thomas Gaisser[a,*] **and Stef Verpoest**[b]

[a] *Bartol Research Institute, Dept. of Physics & Astronomy*
University of Delaware, Newark, DE, USA
[b] *University of Gent, Dept. of Physics and Astronomy,*
B-9000, Gent, Belgium
E-mail: gaisser@udel.edu, stef.verpoest@ugent.be

Competition between decay and re-interaction of charged pions and kaons depends on the temperature/density profile of the upper atmosphere. The amplitude and phase of the variations depend on the minimum muon energy required to reach the detector and on muon multiplicity in the detector. Here we compare different methods for characterizing the muon production profile and the corresponding effective temperature. A muon production profile based on a parameterization of simulations of muons as a function of primary energy is compared with approximate analytic solutions of the cascade equation integrated over primary energy. In both cases, we compare two definitions of effective temperature. We emphasize applications to compact underground detectors like MINOS and OPERA, while indicating how they relate to extended detectors like IceCube.

37th International Cosmic Ray Conference (ICRC 2021)
July 12th – 23rd, 2021
Online – Berlin, Germany

*Presenter

PoS(ICRC2021)1202

1. Introduction

Two-body decays of $\pi^{\pm}$ and $K^{\pm}$ are the principal source of atmospheric muons in the TeV energy range relevant for this paper, where the focus is on inclusive rates of muons from the steep spectrum of all cosmic rays. Prompt muons from decay of charm and three-body decays of kaons [1] contribute significantly only at much higher energies, for example when primary energies in the PeV region and above can be selected by a surface array. The relation of the muon rate to atmospheric temperature evolves over a range determined by the critical energies for decay of the parent mesons, $\epsilon_\pi = 115$ GeV, and $\epsilon_K = 857$ GeV. At the lowest energies both pions and kaons are below the threshold for re-interaction in the atmosphere, so the correlation of the muon rate with temperature is small. Re-interaction becomes significant first for pions and only at higher energy for kaons. Full correlation with temperature is reached for $E_\mu >> 1$ TeV.

The relation between measured muon rate and atmospheric temperature is conventionally quantified by a correlation coefficient, α_T,

$$\frac{\delta R}{R_{av}} = \alpha_T \frac{\delta T}{T_{av}}, \tag{1}$$

where $T = T_{\rm eff}$ and T_{av} is its average over a year and R is the rate of muons. Effective temperature is a convolution of the muon production spectrum as a function of slant depth in the atmosphere with the corresponding temperature profile.

The paper is organized with an initial section on the muon production. We compare approximate analytic solutions of the hadronic cascade equations with a muon production profile characterized by parameters determined from simulation. The next section deals with effective temperature and compares two approaches for relating temperature to muon production. Finally, we discuss calculation of the correlation coefficient, its evolution with energy and how it varies between the different approaches to calculation of rates and effective temperature.

2. Rates of muons

The rate of muons of energy E_μ from a direction θ, ϕ in a detector with effective area $A_{\rm eff}$ is given by

$$\mathrm{R}(\theta,\phi) = \int \mathrm{d}X \int_{E_{\mu,min}} \mathrm{d}E_\mu \, A_{\rm eff}(E_\mu,\theta,\phi) P(E_\mu,\theta,X), \tag{2}$$

where $P(E_\mu,\theta,X)$ is the production spectrum of muons differential in slant depth X. For a compact detector at a depth large compared to its vertical dimension, the effective area is the projected physical area from the direction θ, ϕ. For simplicity, we consider detectors with a flat overburden, in which case the physical area of the detector averaged over azimuth can be used and

$$\begin{aligned} \mathrm{R}(\theta) &= A_{\rm eff}(\theta) \int \mathrm{d}X \int_{E_{\mu,min}} \mathrm{d}E_\mu \, P(E_\mu,\theta,X) \\ &= A_{\rm eff}(\theta) \int \mathrm{d}X P(> E_{\mu,min},\theta,X) \\ &= A_{\rm eff}(\theta) \, I(E_{\mu,min},\theta), \end{aligned} \tag{3}$$

where $I(E_{\mu,min},\theta)$ is the integral muon flux for a given zenith angle and $E_{\mu,min}(\theta)$ is determined by the muon energy-loss formula and the slant depth through the overburden for each zenith angle. In both cases, the total rate is given by

$$\text{Rate} = \sum_{\theta} \text{R}(\theta). \tag{4}$$

Here we use calculations for the MINOS Far Detector (FD) at Soudan [2] and the MINOS ND at Fermilab [3] to compare two approaches to calculating the integral muon flux and its dependence on atmospheric temperature in two different ranges of energy. The standard approach is to use an analytic approximation for the integral flux of muons at slant depth X

$$P(>E_{\mu,min},\theta,X) = F(E_\mu)\frac{A_{\pi\mu}(X)}{\gamma+(\gamma+1)B_{\pi\mu}(X)E_\mu\cos\theta/\epsilon_\pi}, \tag{5}$$

where $F(E_\mu) \equiv E_\mu\, N_0(E_\mu)$, and $N_0(E_\mu) = C\times E_\mu^{-(\gamma+1)}$ is the primary spectrum of nucleons per GeV m^{2}s sr evaluated at the energy of the muon. The integral spectral index is $\gamma \approx 1.7$, This form (plus the corresponding term for kaons) provides the production profile that can be inserted into Eq. 3 to get the integral spectrum of muons. The analytic form 5 is based on a solution [4] to the cascade equation for nucleons, pions and kaons in the atmosphere and produces an inclusive muon flux that is not applicable to multiple muons. The primary spectrum is integrated assuming scaling for the production cross sections and a constant spectral index and appears in Eq. 5 evaluated at the energy of the muon. The production cross sections and two-body decays of the charged pions and kaons appear as spectrum weighted moments for production and decay in the quantities A and B in Eq. 5:

$$A_{\pi\mu}(X) = \frac{Z_{N\pi}}{\lambda_N(\gamma+1)}\frac{1-r_\pi^{\gamma+1}}{1-r_\pi}e^{-X/\Lambda_N}, \tag{6}$$

and

$$B_{\pi\mu}(X) = \frac{\gamma+2}{\gamma+1}\frac{1-r_\pi^{\gamma+1}}{1-r_\pi^{\gamma+2}}\frac{X}{\Lambda^*}\frac{e^{-X/\Lambda_N}}{e^{-X/\Lambda_\pi}-e^{-X/\Lambda_N}}, \tag{7}$$

where $\Lambda_\pi^* = \Lambda_\pi\times\Lambda_N/(\Lambda_\pi-\Lambda_N)$ is a combination of the attenuation lengths for nucleons and pions. The equations for the kaon channel have the same form, with the branching ratio 0.635 multiplying $A_{K\mu}(X)$. For calculations we use the TeV values of spectrum-weighted moments and attenuations lenghts from Ref. [4].

An alternate approach is to use a parameterization of Monte Carlo simulations to calculate $P(>E_{\mu,min},\theta,X)$. In this case, because the simulation is following the production of muons along the trajectory of the primary cosmic ray, multiple muons are included. In Ref. [5] the parameterization was applied to the seasonal variation of multiple muon events as measured by MINOS [6] and by the NOvA ND [7]. Here we use it to calculate total rates of muons integrated over the primary spectrum. Because the total rates are dominated by single muons, the comparison with the analytic approach is of interest. For the primary spectrum in both cases we use the primary spectrum of nucleons from the H3a model [8, 9] of the spectrum and composition for the calculations shown below.

Table 1 shows the binning in zenith angle and the corresponding minimum muon energies used to calculate total rates (Eq. 4). The corresponding angular distributions are shown in Fig. 1. The

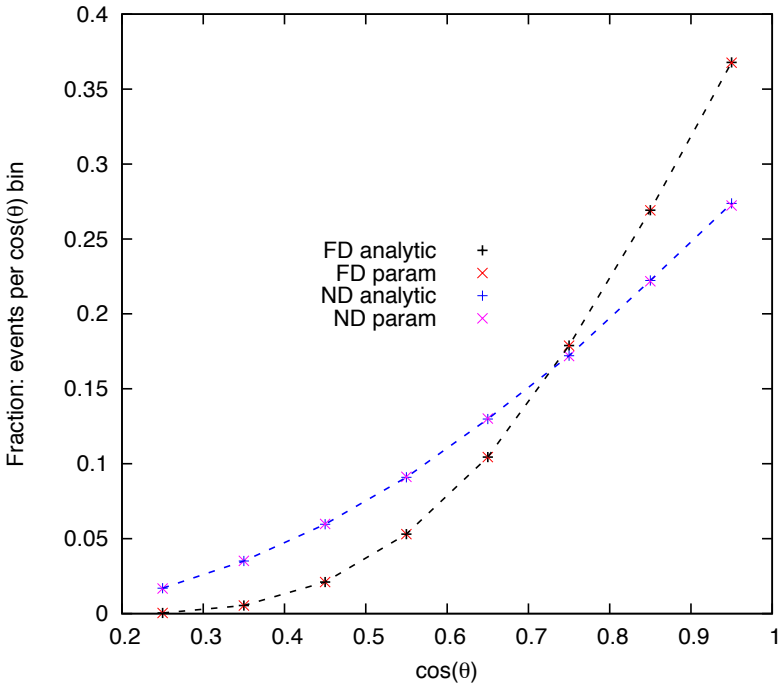

Figure 1: Angular distribution the the MINOS near a far detectors.

distribution is significantly flatter for the shallow detector at Fermilab where the muons of lower energy are not so much influenced by radiative energy losses as for the deep detector at Soudan.

Table 1: Minimum muon energies (GeV) for 8 bins of $\cos\theta$

$\cos\theta$	0.95	0.85	0.75	0.65	0.55	0.45	0.35	0.25
MINOS FD	730	850	1030	1320	1800	2730	5000	14000
MINOS ND	50	56	64	74	89	111	147	217

3. Effective temperature

The effective temperature is a convolution of the atmospheric temperature profile with muon production along a path defined by the zenith angle. One possibility is to define it as

$$T_{\rm eff}(\theta) = \frac{\int {\rm d}X\, P(E_\mu, \theta, X)\, T(X)}{\int {\rm d}X\, P(E_\mu, \theta, X)}, \tag{8}$$

A simple derivation of a different definition of effective temperature starts by taking the variance of the rate with respect to temperature.

$$\begin{aligned} \Delta{\rm R}(\theta) \quad &= \quad \int {\rm d}X \int {\rm d}E_\mu\, A_{\rm eff}(E_\mu, \theta) \\ &\times \frac{{\rm d}P(E_\mu, \theta, X)}{{\rm d}T} \Delta T. \end{aligned} \tag{9}$$

Then define $\Delta T = T(X) - T_{\rm eff}$ and set $\Delta \mathrm{R} = 0$ to get

$$T_{\rm eff}(\theta) = \frac{\int \mathrm{d}X \int \mathrm{d}E_\mu \, A_{\rm eff}(E_\mu, \theta) T(X) \frac{\mathrm{d}P(E_\mu, \theta, X)}{\mathrm{d}T}}{\int \mathrm{d}X \int \mathrm{d}E_\mu \, A_{\rm eff}(E_\mu, \theta) \frac{\mathrm{d}P(E_\mu, \theta, X)}{\mathrm{d}T}}. \tag{10}$$

This derivative definition of effective temperature originated with the first paper on seasonal variations of muons [10], and a more recent implementation [11] is used by MINOS and detectors such as OPERA [12] at LNGS. Use of the simple analytic approximation of Eq. 5 leads to relatively simple forms listed in the next paragraph. Application to the parameterization requires numerical differentiation of $P(> E_\mu, \theta, Z)$.

The temperature dependence of the muon production spectrum is entirely contained in the two critical energies,

$$\epsilon_i = \frac{m_i c^2}{c\tau_i} \frac{RT}{Mg} \text{ with } \frac{RT}{Mg} = 29.62 \, \frac{\mathrm{m}}{^\circ K}. \tag{11}$$

Thus, for the differential form of the pion channel, for example,

$$T(X) \frac{dP(E_\mu, \theta, X)}{dT} = \frac{A_{\pi\mu}(X) B_{\pi\mu}(X) E_\mu \cos\theta / \epsilon_\pi(T)}{[1 + B_{\pi\mu} E_\mu \cos\theta / \epsilon_\pi(T)]^2}. \tag{12}$$

The corresponding integral form is

$$T_{\rm eff}(\theta) = \frac{\int \mathrm{d}X \, T(X) \frac{\mathrm{d}P(>E_\mu, \theta, X)}{\mathrm{d}T}}{\int \mathrm{d}X \, \frac{\mathrm{d}P(>E_\mu, \theta, X)}{\mathrm{d}T}}, \tag{13}$$

with

$$T(X) \frac{dP(> E_\mu, \theta, X)}{dT} = \frac{A_{\pi\mu}(X)(\gamma+1) B_{\pi\mu}(X) E_\mu \cos\theta / \epsilon_\pi(T)}{[\gamma + (\gamma+1) B_{\pi\mu} E_\mu \cos\theta / \epsilon_\pi(T)]^2}. \tag{14}$$

It is enlightening to apply the two definitions of effective temperature to calculation of the correlation between rate and $T_{\rm eff}$. Figure 2 shows the correlation from the analytic calculation for the MINOS FD. The same comparison using the parameterization is shown in Fig. 3. The corresponding correlations for the MINOS ND are presented in Figs. 4 and 5.

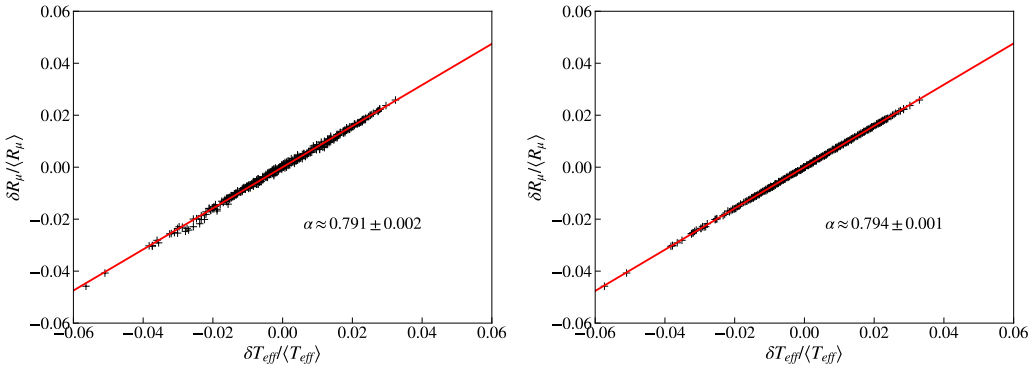

Figure 2: Correlation with temperature for the MINOS FD calculated with the analytic formula; Left: T1 and Right: T2.

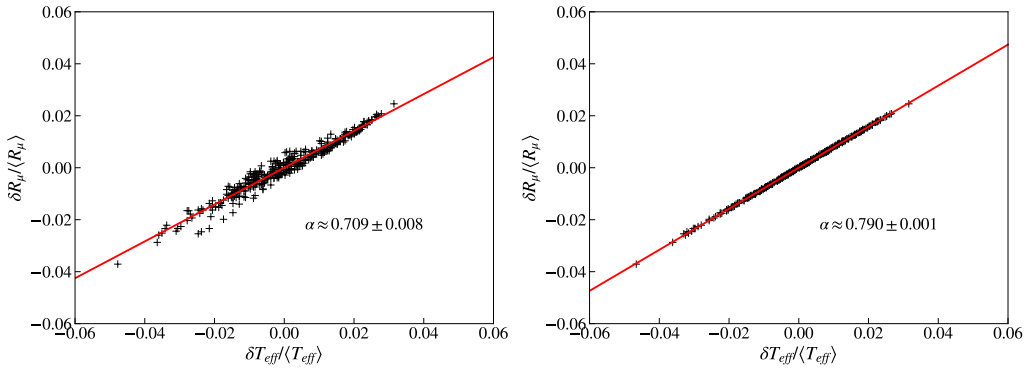

Figure 3: Correlation coefficient for the MINOS FD calculated with the parameterization; Left: T1 and Right: T2.

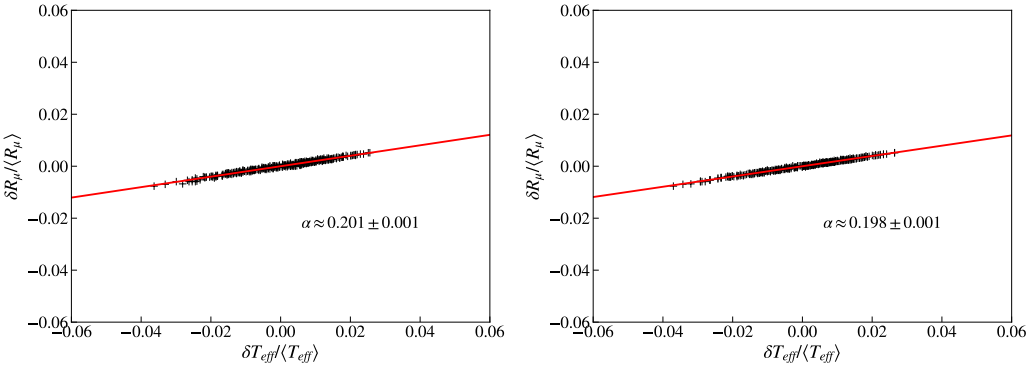

Figure 4: Correlation with temperature for the MINOS ND calculated with the analytic formula; Left: T1 and Right: T2.

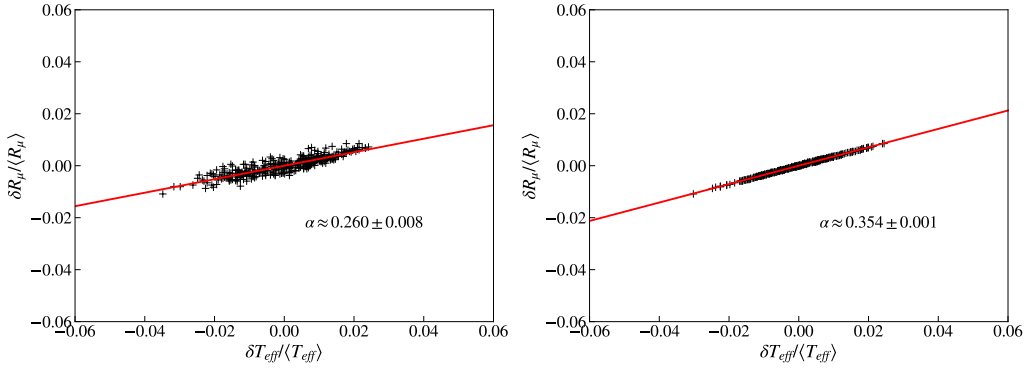

Figure 5: Correlation coefficient for the MINOS ND calculated with the parameterization; Left: T1 and Right: T2.

4. Correlation coefficient

Slopes of straight-line fits to the data shown in the correlation plots give the respective coefficients, α_T from Eq. 1, for each set of assumptions. In all cases, the derivative definition of effective temperature (Eq. 10) gives a tighter correlation with the fit line. This reduction of scatter is especially noticeable when the rates are calculated with the parameterization. For the MINOS ND the measured correlation coefficient is $\alpha_T = 0.352 \pm 0.046$ [3], and for the FD $\alpha_T = 0.873$ [2]. It should be emphasized, however, that these are correlations with measured rates, whereas the figures here show correlations with calculated rates. For the MINOS FD, all the calculations give coefficients somewhat below the measured value. It is interesting that for the shallow detector, the experimental value is closer to the result when the rates are calculated with the parameterization.

5. Summary

Understanding seasonal variations of muon rates in underground detectors requires accounting for the temperature profile in the integration of the muon production spectrum over slant depth in the atmosphere. This paper compares two approaches to calculation of rates in compact underground detectors: 1) uses an analytic approximation to the muon production spectrum as a function of slant depth in the atmosphere and 2) uses a formula based on simulations. In both cases, the temperature-dependence is entirely contained in the critical energies for pions and kaons. Results are typically quantified as the correlation between the muon rate and a single effective temperature evaluated for each day (or other time span) for which the rates are determined, either by calculation or by measurement. We compared two definitions of $T_{\rm eff}$, one in which temperature is weighted by the muon production spectrum itself, and another in which it is weighted with the derivative with respect to temperature of the production spectrum. The latter has been traditionally used in analysis of results from compact underground detectors. By definition it minimizes deviation of calculated rates from the value expected for a given effective temperature.

These different methods are illustrated in two different energy ranges by calculations for the MINOS ND ($E_\mu \sim 100$ GeV) and for the MINOS FD ($E_\mu \sim 1$) TeV. As expected, the correlation with effective temperature is significantly higher ($\alpha_T \sim 0.79$) for the higher energy region than for lower energies (0.2 to 0.35). In the lower energy range, with $E_\mu \sim \epsilon_\pi$, the dominant pion component still has a high probability to decay, whereas in the higher energy range it is fully correlated with the temperature.

One aspect that remains to be examined is the relation between the fractional contribution of the kaon channel to the calculated rates and the values of the corresponding correlation coefficients. Other things being equal, a larger kaon fraction should result in a smaller value of the correlation coefficient. The opposite is the case for the lower energy calculation, where the kaon fraction is higher for the parameterization, but the correlation coefficient is higher.

References

[1] T. K. Gaisser and S. R. Klein, *Astropart. Phys.* **64** (2015) 13–17.

[2] **MINOS** Collaboration, P. Adamson et al., *Phys. Rev.* **D81** (2010) 012001.

[3] P. Adamson et al., *Phys. Rev.* **D90** (2014) 012010.

[4] T. K. Gaisser, R. Engel, and E. Resconi, *Cosmic Rays and Particle Physics*. Cambridge University Press, 2016.

[5] T. K. Gaisser and S. Verpoest, arXiv:2106.12247.

[6] **MINOS** Collaboration, P. Adamson et al., *Phys. Rev.* **D91** (2015) 112006.

[7] **NOvA** Collaboration, M. A. Acero et al., *Phys. Rev.* **D99** (2019) 122004.

[8] T. K. Gaisser, *Astropart. Phys.* **35** (2012) 801–806.

[9] T. K. Gaisser, T. Stanev, and S. Tilav, *Front. Phys. (Beijing)* **8** (2013) 748–758.

[10] P. Barrett et al., *Rev. Mod. Phys.* **24** (1952) 133–178.

[11] E. Grashorn, J. de Jong, M. Goodman, A. Habig, M. Marshak, S. Mufson, S. Osprey, and P. Schreiner, *Astropart. Phys.* **33** (2010) 140–145.

[12] **OPERA** Collaboration, N. Agafonova et al., *JCAP* **10** (2019) 003.